Observation of Discrete Surface Solitons

S. Suntsov, K. G. Makris, D. N. Christodoulides, and G. I. Stegeman
College of Optics and Photonics, CREOL & FPCE, University of Central Florida, 4000 Central Florida Boulevard, Orlando, Florida 32816, USA

A. Haché
Département de physique et d'astronomie, Université de Moncton, E1A 3E9 Canada

R. Morandotti
Institut national de la recherché scientifique, Université du Québec, Varennes, Québec, J3X 1S2 Canada

H. Yang and G. Salamo
Physics Department, University of Arkansas, Fayetteville, Arkansas 72701, USA

M. Sorel
Department of Electrical and Electronic Engineering, University of Glasgow, Glasgow G12 8QQ, Scotland, United Kingdom
(Received 3 July 2005; published 13 February 2006)

We report the first observation of discrete optical surface solitons at the interface between a nonlinear self-focusing waveguide lattice and a continuous medium. The effect of power on the localization process of these optical self-trapped states at the edge of an AlGaAs waveguide array is investigated in detail. Our experimental results are in good agreement with theoretical predictions.

DOI: 10.1103/PhysRevLett.96.063901 PACS numbers: 42.65.Tg, 42.65.Sf, 42.82.Et

Surfaces waves are known to display properties that have no analogue in the bulk [1]. Over the years, this ubiquitous class of waves has been the subject of intense study in diverse areas of physics, chemistry, and biology. In condensed matter physics, quantum surface states were first predicted by Tamm in 1932 by considering the neglected edge effects in a semi-infinite Kronig-Penney model [2]. Subsequently, Shockley showed how such states can emerge from atomic orbitals and demonstrated that the associated surface levels can lead to surface bands in three dimensional crystals [3,4]. In general, these surface waves arise from the abrupt break in translational symmetry and are localized at the interface (with exponentially decaying probability) in both the outer and inner region of the crystal. In linear optics, Tamm-Shockley-like surface waves were suggested in periodic media [5] and were successfully observed in AlGaAs multilayer structures [6,7]. Unlike plasmon-polariton waves [8] that are tightly bound to a metal surface, optical surface waves in periodic lattices are confined due to the fact that their propagation eigenvalues fall within the forbidden band gaps of the system [7].

In nonlinear optics, nonlinear surface waves have also been extensively studied [9–15]. In particular, nonlinear TE, TM, and mixed-polarization surface waves traveling along single dielectric interfaces were theoretically predicted and analyzed in several works [9]. These waves are a direct outcome of nonlinearity and have no analogue whatsoever in the linear domain. This is exemplified in the case of nonlinear TE surface waves that cannot exist under linear conditions at the interface of two dielectric media [10,11]. The stability of these waves at a single interface was also investigated [12]. Yet, so far, direct observation of these nonlinear optical surface waves has been hindered by experimental difficulties (because of proper excitation, high power thresholds, etc.). As a result, most of the activity in this area has remained theoretical. Clearly, it is of interest to develop new configurations capable of supporting this family of waves.

In the past few years, discreteness in nonlinear periodic systems has opened up unique opportunities for observing new phenomena that are by their nature impossible in continuous media [16]. A prime example of such a nonlinear discrete structure is that of an array of evanescently coupled optical waveguides. Discrete solitons and modulational instability [17,18], anomalous diffraction and diffraction management [19], as well as incoherent self-trapped waves, have been observed in Kerr, photorefractive, quadratic, and liquid crystal nonlinear waveguide lattices [20,21]. Quite recently, the possibility of discrete surface solitons in 1D array structures has been theoretically predicted [22]. These self-localized states are located at the edge of a semi-infinite array and exhibit a power threshold property similar to that encountered by nonlinear surface waves at an interface between continuous media. Hence, this approach may be utilized to experimentally explore the dynamical behavior of nonlinear surface waves. Observation of such interface solitons would open the way to study surface soliton interactions, their instabilities, new ways to implement nonlinear spectroscopies specific to interfaces, defect effects, etc.

In this Letter, we report the first experimental observation of discrete surface solitons at the interface between a Kerr-nonlinear AlGaAs waveguide lattice and a continuous medium. This approach is attractive because the power response is determined by two easily controllable fabrication parameters, namely, the difference between the propagation constants of the channels and the continuous region, and the coupling strength between adjacent waveguides. The effect of power on the localization process of these optical self-trapped states at the edge of the waveguide array is investigated in detail. The experimental results are in very good agreement with theoretical predictions.

To gain an understanding of the properties of surface discrete solitons in semi-infinite self-focusing waveguide arrays we employ here the tight-binding approximation. The normalized modal optical field amplitudes evolve according to a discrete nonlinear Schrödinger-like equation [17], i.e.,

$$i\frac{da_0}{dZ} + a_1 + |a_0|^2 a_0 = 0, \tag{1a}$$

$$i\frac{da_n}{dZ} + (a_{n+1} + a_{n-1}) + |a_n|^2 a_n = 0 \tag{1b}$$

where Eq. (1a) describes the field at the edge of the array ($n = 0$ waveguide site) and Eq. (1b) applies at every other site $n \geq 1$. The normalized coordinate Z is given by $Z = \kappa z$, where z is the actual propagation distance and κ is the coupling coefficient between adjacent waveguide sites. The actual electric fields E_n are related to the dimensionless amplitudes a_n through the relation $E_n = (2\kappa\lambda_0\eta_0/\pi n\hat{n}_2)^{1/2} a_n$, where λ_0 is the free space wavelength, η_0 is the free space impedance, $\hat{n}_2$ is the nonlinear Kerr coefficient, and n refers to the linear refractive index of the array. Under linear conditions, the spatial impulse response of this semi-infinite system can be obtained in closed form in terms of Bessel functions [22].

Nonlinear discrete surface waves in a semi-infinite array can be numerically found using relaxation methods by assuming a stationary solution of the form $a_n = u_n \exp(i\mu Z)$ in Eqs. (1), where $\mu \geq 2$ represents the change in the propagation eigenvalue due to the nonlinearity. Because the nonlinearity is of the self-focusing type, here we are only searching for in-phase solutions, i.e., all the fields u_n are taken to be positive [22]. The interface soliton properties discovered there mirrored closely the characteristic of surface solitons between continuous media [9–14]. Namely, there is a power threshold for existence, a stable branch in which the localization increases with power and the evanescent field decays into the lower-index medium. In fact, as shown in Fig. 1 similar results can be obtained for surface soliton fields localized at the $n = 1$ and 2 channels. For illustration purposes the amplitudes a_n have been multiplied by the mode profile. The field is asymmetric around the maximum, and this asymmetry vanishes as the localization site n of the solution moves inside the array, away from the interface ($n \gg 1$). This is anticipated, since for large values of n, the well-known symmetric discrete soliton is obtained. Furthermore, the power threshold characteristic of surface solitons goes to zero as n (the site where the soliton peak resides) increases. Moreover, numerical simulations reveal that unstable surface solitons that reside in the n channel eventually drop into the $n + 1$ site due to instabilities. Intuitively, this should have been expected since for every unstable solution at the n site, there always exists a stable solution of a lower power at the $n + 1$ waveguide.

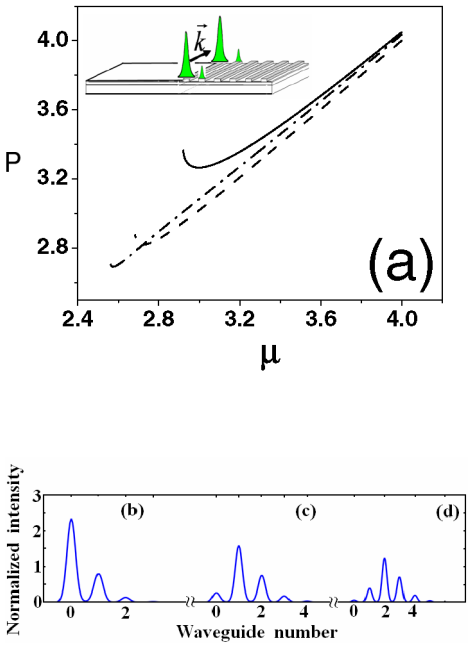

FIG. 1 (color online). (a) Normalized discrete surface soliton power P versus the normalized eigenvalue μ, where every line corresponds to a different soliton solution. The maximum of the field occurs at the $n = 0$ waveguide site (solid line), $n = 1$ waveguide site (dashed line), and $n = 2$ waveguide site (dash-dot line). (b), (c) and (d) show the normalized intensity profiles when the maximum is at $n = 0$, $n = 1$, and $n = 2$ waveguide sites, respectively. The inset in (a) depicts the array interface.

We would like to emphasize that in the linear regime the lattice system under consideration cannot support any linear surface waves since the background refractive index of the array is the same as that of the outer slab region.

Given the fact that our experiments utilized ultrashort pulses and that the waveguides are not only dispersive but also exhibit three-photon absorption, we have simulated the beam dynamics in both space and time. The underlying nonlinear Schrödinger equation that describes this one-dimensional AlGaAs system is

$$i\frac{\partial U}{\partial z} + \frac{1}{2k}\frac{\partial^2 U}{\partial x^2} - \frac{k''}{2}\frac{\partial^2 U}{\partial T^2} + k_0\delta f(x)U + k_0 n_2|U|^2 U + ia|U|^4 U = 0, \tag{2}$$

where U is the envelope of the optical field, x is the transverse axis, and T is a time coordinate moving at the group velocity of the wave. The second term in Eq. (2) describes the spatial diffraction process, the third is associated with dispersion effects, while the fifth one accounts for the Kerr nonlinearity. The term associated with the normalized periodic potential $f(x)$ arises from the periodicity of the array. In addition, $k_0 = 2\pi/\lambda_0$, $k = k_0 n$ (where the refractive index of AlGaAs $n = 3.28$) is the propagation wave vector, $k'' = 1.3 \times 10^{-24}$ m^{-1} s^2 is the normal dispersive coefficient of the material, $\delta = 1.5 \times 10^{-3}$ is the index difference between the core and the cladding regions in the array, and $n_2 = \hat{n}_2 n/2\eta_0$ where $\hat{n}_2 = 1.5 \times 10^{-13}$ cm^2/W is the Kerr nonlinearity. Finally, three-photon absorption has been included in the last term of Eq. (2), where $a = \alpha_3 n^2/8\eta_0^2$, with $\alpha_3 = 0.04$ cm^3/GW^2.

The actual sample structure used in the experiments is shown in Fig. 2(a). The material and structural parameters are close to those previously used to observe discrete, highly localized Kerr solitons inside the structure [23]. The array contained 101 channels and was 1 cm long. The coupling length was measured to be 2.2 mm by fitting

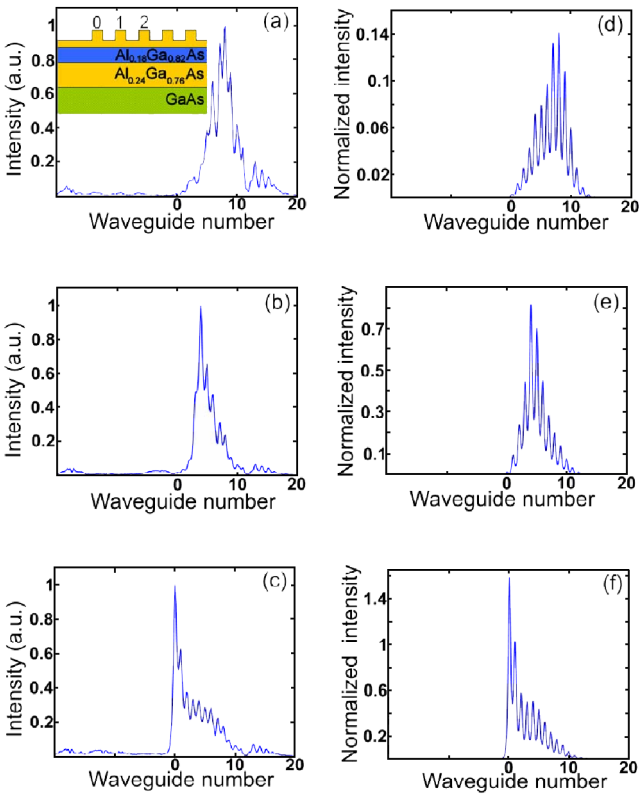

FIG. 2 (color online). Intensity patterns observed at the output of the AlGaAs array for single channel excitation at three different peak input power levels injected into channel $n = 0$. Left-hand side: experimental results for (a) $P = 450$ W; (b) $P = 1300$ W; (c) $P = 2100$ W. Right-hand side: numerical calculation results for (d) $P = 280$ W; (e) $P = 1260$ W; (f) $P = 2200$ W. The inset shows the actual sample geometry.

the linear diffraction pattern inside the array with that anticipated from theory.

The experimental apparatus for the observation of surface discrete solitons was similar to that used for observation of discrete modulational instability [18], with the principal difference being that the only one arm of the layout was utilized to inject the beam into AlGaAs waveguide array. In brief, a 1 kHz train of 1 ps pulses at 1550 nm from an optical parametric amplifier was focused onto the entrance facet of the waveguide array at and near the first channel [labeled "0" in the inset of Fig. 2(a)]. The input intensity distribution was shaped by a lens train to be close to that of the fundamental mode supported by a single channel. The shape, measured at the output of a single isolated waveguide, was elliptical with full-width-at-half-intensity dimensions of 7×2.5 μm (effective area of the mode). The output intensity distribution for various excitation conditions was imaged on an InGaAs line array camera (Roper-Scientific OMA-V). The total power of both input and output beams was measured with calibrated germanium photodiodes.

The first set of experiments and simulations dealing with optimum excitation of the $n = 0$ channel are depicted in Fig. 2. Results at three different excitation powers are shown. The lowest power corresponds to linear diffraction [Figs. 2(a) and 2(d)], the second to intermediate power levels [Figs. 2(b) and 2(e)] (partial collapse of this diffraction pattern towards a discrete surface soliton), and the third [Figs. 2(c) and 2(f)] to the intensity distribution of a discrete surface soliton. Even though the experiments were carried out with pulses, a rapid collapse of the output pattern into a discrete soliton was found to occur after 1.7 kW, thus supporting the existence of a power threshold. The theoretical Figs. 2(d)–2(f) depict integrated intensities ($\propto \int |U|^2 dT$) since the photodiode response depends only on photon energy. Overall the agreement between experiment and theory is very good. The fields decay exponentially into the continuous region. In the second and third cases the long "tails" trailing into the array from the $n = 0$ channel are a consequence of the temporal pulse excitation. For example, for the highest power case, the intermediate instantaneous powers associated with the pulse lead to only partial collapse while the low power tails produce the equivalent of the linear discrete diffraction pattern. In Fig. 2 one can also observe some weak, diffracting radiation in the continuous region due to imperfect excitation of the first $n = 0$ channel. In fact, when the center of the incident beam is moved to partially overlap the $n = 0$ channel and the continuum, sufficient power is radiated into the continuous slab to also initiate beam collapse into a spatial soliton there.

Further experiments with the excitation of other channels close to the edge of the waveguide array were conducted. Figure 3 shows the output intensity profiles for the third ($n = 2$) channel excitation for three different input

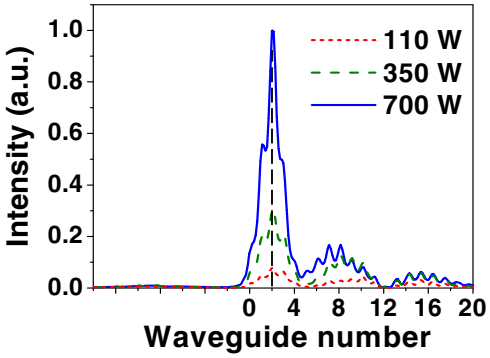

FIG. 3 (color online). Intensity patterns observed at the output of the AlGaAs array for single channel excitation of the third ($n = 2$) channel for three different input peak power levels.

power levels. As power is increased, the diffraction pattern again collapses into a surface soliton with an asymmetric field profile centered at the ($n = 2$) waveguide. Similar behavior was observed in the experiments with the excitation of second ($n = 1$) and fourth ($n = 3$) channels.

Another set of experiments was done using wide strongly asymmetric beam excitation (intensity profile FWHM of 50 μm) injected into two different positions of the AlGaAs array with the maximum of the beam profile in the middle of the array [Fig. 4(a)], and the maximum located at the first ($n = 0$) channel [Fig. 4(b)]. This beam profile asymmetry with its steep side facing the edge of the array was chosen to prevent a significant amount of radiation from leaking into the continuum region. Output intensity patterns for three different input power levels are presented for each arrangement. Figure 4(a) shows that, as power is increased, the output diffraction pattern in the middle of the array forms a discrete soliton centered at two channels away from the position of the maximum of input beam, near the centroid position of the input energy. Unlike this, in Fig. 4(b), a discrete surface soliton is formed at the

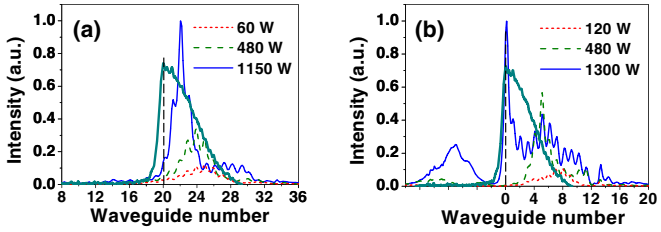

FIG. 4 (color online). Intensity patterns observed at the output of AlGaAs array for wide asymmetric beam excitation. (a) Beam is injected in the middle of the array; (b) Peak of the input beam profile is at the first ($n = 0$) channel site. Output patterns for three different input peak power levels for each case are shown. The thick solid (green oline) line represents the intensity profile of the input beam. The vertical dashed line shows the position of the input beam peak.

first channel site, corresponding to the peak of the input beam. This proves that the surface discrete solitons are indeed the nonlinear eigenmodes near the interface.

In summary, we report the first experimental observation of optical discrete surface solitons.

[1] A. Zangwill, *Physics at Surfaces* (Cambridge University Press, Cambridge, New York, 1988).
[2] I. Tamm, Phys. Z. Sowjetunion **1**, 733 (1932).
[3] W. Shockley, Phys. Rev. **56**, 317 (1939).
[4] S. G. Davison and M. Steslicka, *Basic Theory of Surface States* (Oxford University Press, New York, 1992).
[5] D. Kossel, J. Opt. Soc. Am. **56**, 1434 (1966); J. A. Arnaud and A. A. Saleh, Appl. Opt. **13**, 2343 (1974).
[6] P. Yeh, A. Yariv, and A. Y. Cho, Appl. Phys. Lett. **32**, 104 (1978).
[7] P. Yeh, A. Yariv, and C. S. Hong, J. Opt. Soc. Am. **67**, 423 (1977).
[8] W. L. Barnes, A. Dereux, and T. W. Ebbesen, Nature (London) **424**, 824 (2003).
[9] A. D. Boardman, P. Egan, F. Lederer, U. Langbein, and D. Mihalache, *Nonlinear Surface Electromagnetic Phenomena*, edited by H. E. Ponath and G. I. Stegeman (North-Holland, Amsterdam, 1991), Vol. 29, p. 73.
[10] M. Miyagi, and S. Nishida, Sci. Rep. Res. Inst. Tohoku Univ. Ser. B **24**, 53 (1972).
[11] W. J. Tomlinson, Opt. Lett. **5**, 323 (1980).
[12] N. N. Akhmediev *et al.*, Sov. Phys. JETP **61**, 62 (1985).
[13] U. Langbein, F. Lederer, and H. E. Ponath, Opt. Commun. **46**, 167 (1983).
[14] C. T. Seaton, J. D. Valera, R. L. Shoemaker, G. I. Stegeman, J. T. Chilwell, and S. D. Smith, IEEE J. Quantum Electron. **21**, 774 (1985).
[15] M. Cronin-Golomb, Opt. Lett. **20**, 2075 (1995).
[16] D. N. Christodoulides, F. Lederer, and Y. Silberberg, Nature (London) **424**, 817 (2003).
[17] D. N. Christodoulides and R. I. Joseph, Opt. Lett. **13**, 794 (1988); H. S. Eisenberg *et al.*, Phys. Rev. Lett. **81**, 3383 (1998).
[18] J. Meier *et al.*, Phys. Rev. Lett. **92**, 163902 (2004).
[19] H. S. Eisenberg *et al.*, Phys. Rev. Lett. **85**, 1863 (2000); M. J. Ablowitz and Z. H. Musslimani, Phys. Rev. Lett. **87**, 254102 (2001).
[20] J. W. Fleischer *et al.*, Nature (London) **422**, 147 (2003); N. K. Efremidis *et al.*, Phys. Rev. E **66**, 046602 (2002); O. Cohen *et al.*, Nature (London) **433**, 500 (2005); D. Neshev *et al.*, Opt. Lett. **28**, 710 (2003).
[21] R. Iwanow *et al.*, Phys. Rev. Lett. **93**, 113902 (2004); A. Fratalocchi *et al.*, Opt. Lett. **29**, 1530 (2004); Y. V. Kartashov *et al.*, Opt. Lett. **30**, 637 (2005); H. Martin *et al.*, Phys. Rev. Lett. **92**, 123902 (2004); B. A. Malomed and P. G. Kevrekidis, Phys. Rev. E **64**, 026601 (2001).
[22] K. G. Makris, S. Suntsov, D. N. Christodoulides, G. I. Stegeman, and A. Hache, Opt. Lett. **30**, 2466 (2005).
[23] J. Meier *et al.*, Phys. Rev. Lett. **91**, 143907 (2003).